J. Phys. B: At. Mol. Opt. Phys. **29** (1996) 2265–2287. Printed in the UK

The separable representation of exchange in electron–molecule scattering: I. Elastic scattering and rotational excitation

Grahame Danby†, Brian K Elza‡, Michael A Morrison§ and Wayne K Trail§

† Department of Physics and Astronomy, University College London, London WC1E 6BT, UK

‡ HUGHES STX, 4400 Forbes Blvd, Lanham, MD 20706, USA

§ Department of Physics and Astronomy, University of Oklahoma, Norman, OK 73019-0225, USA

Received 3 August 1995, in final form 14 February 1996

Abstract. We have investigated a systematic procedure for representing, as a separable expansion, the exchange interaction in electron–molecule scattering. Illustrative calculations of scattering quantities (eigenphase sums, total cross sections and rotationally-resolved differential cross sections) have been performed for electron scattering from molecular hydrogen in the fixed-nuclear-orientation approximation. The exchange basis can be constructed from the same Cartesian Gaussian functions used to generate the near-Hartree–Fock static interaction, supplemented by an even-tempered series of Gaussian functions located on the molecular centre of mass. Particular emphasis is placed on examining the convergence properties of this series.

1. Introduction

A major obstacle to the accurate calculation of low-energy electron–molecule scattering cross sections is the non-local part of the interaction potential that arises from exchange and bound–free correlation effects. These interactions significantly increase the computational demands incurred by solution of the Schrödinger equation. One approach, which is capable of yielding useful results, is to adopt a physically realistic local model potential (Morrison and Collins 1978). For electronically elastic collisions, such a model must include firstly the local static interaction between the incoming electron and the ground state of the target molecule. The non-local exchange potential can be viewed as a correction to this static potential due to the imposition of antisymmetry on the total electronic wavefunction describing the scattered electron plus target electrons. This enforcement of the Pauli exclusion principle keeps apart electrons of like spin and is described by an exchange interaction, the isotropic component of which should be attractive (Hara 1967). Local exchange potentials, for example those based on treating the target electrons as a free-electron gas, demonstrate this property (Morrison and Trail 1993). Model exchange potentials have been used in the study of electronically elastic collisions of electrons with a range of diatomic (Morrison and Collins 1981, Trail *et al* 1990) and polyatomic (Collins and Morrison 1982, Jain *et al* 1991) molecules. The omission of electronically excited states can be compensated for, at energies below the first electronic inelastic threshold, by the addition of a third component to the interaction potential which allows for target distortion. One example is the BTAD (better than adiabatic dipole) polarization potential used in the

0953-4075/96/112265+23$19.50

present work (Gibson and Morrison 1984). This ignores velocity-dependent effects and further applies a non-penetrating approximation to the incident electron. There will always be systems for which such departures from full *ab initio* rigour are unavoidable with existing computer facilities.

For large polyatomic molecules with many electrons it would be reasonable to apply in the first instance a simple free-electron gas exchange potential. More accurate results could be obtained by 'tuning' the potential by, for example, treating the target ionization potential as a parameter in a way found to be essential for smaller diatomic systems (Morrison and Collins 1981). However, increasing use is being made of separable representations which expand the exchange kernel in terms of products of one-electron functions (Rescigno and Orel 1981). This approach, the focus of the present paper, has the advantage of being a rigorous method of treating exchange while still offering computational savings in the solution of the coupled integrodifferential equations of electron–molecule scattering theory.

For this reason, separable expansions have featured prominently in numerical solutions of the many-particle Schrödinger equation for both bound and continuum states (Yamaguchi 1954, Lovelace 1964). The primary advantage of such expansions is that they dramatically decrease the number of integrals one must evaluate upon introduction of a discrete basis (as in the Schwinger variational calculations of Smith *et al* (1984)) or discrete grid representations (as in the linear algebraic calculations of Collins and Schneider 1981). In electron–molecule scattering calculations, the computational demands imposed by these integral evaluations can be prohibitive, precluding one from studying all but the simplest systems. Hence many investigators have adopted separable representations of non-local potentials in studies that encompass scattering from non-polar diatomics (e.g. e–N_2 in Malegat and Le Dourneuf 1988), polar diatomics (e.g. e–LiH in Rescigno and Orel 1981), linear triatomics (e.g. e–CO_2 in Schneider and Collins 1981a), and, most recently, non-linear polyatomics (e.g. e–CH_4 in Gianturco *et al* 1995).

However, unlike the Hamiltonian in a linear variational optimization of the ground-state energy of a bound system, the exchange kernel for an electron–target system is not governed by a minimum principle. So while the goals in choosing a basis for a separable representation of such a kernel resemble those of bound-state calculations—to span the region of space where the exchange operator influences the scattering function in a way that yields accurate scattering quantities when that function is propagated into the asymptotic region—the lack of a minimum principle eliminates the guarantee that increasing the size of a given basis will lead to improvement (or, at worst, no change) in the quality of the answers. This lack further implies that one cannot be certain that a converged scattering quantity has, in fact, converged to the right answer—unless, of course, one knows the right answer in advance, in which case one does not need a separable representation. The choice of the basis for such a representation, therefore, is a major concern.

This issue becomes especially exigent in studies of vibrational excitation, a scattering process that is almost pathologically sensitive to approximations in the interaction potential, as illustrated in Trail (1991) and Morrison *et al* (1987). Prior theoretical investigations by the University of Oklahoma theory group of vibrational excitation of H_2 by low-energy electrons, aimed at resolving discrepancies between various experimental determinations of cross sections for this process (Morrison *et al* 1987), revealed the sensitivity of this process to exchange and drove us beyond local model potentials to separable representations (Crompton and Morrison 1993) and exact inclusions of this non-local potential (Buckman *et al* 1990), a calculation that to date has been performed only for this system.

This heightened sensitivity as well as the need for high precision calculations and independence from experimental cross section data motivated our investigation of the

accuracy of separable representations of exchange, beginning in the present paper with elastic scattering and rotational excitation and continuing in a subsequent paper with vibrational excitation. This study focuses on two issues: (i) the systematic determination of bases for expansion of the exchange operator without incurring linear dependence, and (ii) the accuracy of scattering quantities obtained by solving the Schrödinger equation with the separated kernel, as determined by comparison to results of exact exchange calculations (Trail 1991). Here we explore the viability of one type of basis for such calculations, based on an 'even-tempered' set of Gaussian-type orbitals. As we shall show in section 3, although one can obtain accurate e–H_2 cross sections and eigenphase sums with such a basis, convergence of these results with respect to the basis does not necessarily ensure that the answer is correct. Hence the intent of this paper is cautionary as well as prescriptive.

An optical potential, constructed from virtual excitations of the target electrons, is a rigorous way of representing polarization and correlation effects (Schneider and Collins 1983). These may also be included in the scattering equations using a separable representation. However, the long-range nature of polarization, in comparison with exchange, is likely to call for a greater number of basis functions, including more diffuse ones. We have been mindful of such future applications when experimenting with the inclusion of diffuse one-electron functions in the separable treatment of exchange.

Historically, work on separable exchange in electron collisions with small molecules (treated as rigid rotors) was extremely encouraging. This work promised high accuracy with small exchange bases and little more computer time than a local potential calculation (Rescigno and Orel 1981, Collins and Schneider 1981). Subsequently, Malegat *et al* (1987) studied the properties of the separable representation for electron–H_2 scattering, examining the convergence behaviour of fixed-nuclei eigenphase sums using four exchange bases.

The work described in the present paper similarly considers the nuclei to be fixed (at their equilibrium separation) but differs from the earlier study in several ways. First, we have calculated benchmark exact-exchange values of the scattering quantities for comparison, using the same target wavefunction and numerical criteria comparable to those of our separable calculations. Malegat *et al* used instead the exact static-exchange cross sections of Collins *et al* (1978, 1980). We have performed new calculations, both at the static-exchange level and including polarization. Given the ongoing theoretical and experimental interest in the e–H_2 system (Buckman *et al* 1990, Rescigno *et al* 1993), it is clearly more pertinent to focus on a full static-exchange-polarization treatment. We have also considered a larger number of basis sets which are, in addition, inter-related by an even-tempered series of Cartesian Gaussian-type orbitals; this is important given the absence of a variational principle for the exchange operator. Furthermore, the use of analytically convenient GTOs is also more relevant (than the Slater-type bases of Malegat *et al*) for future extensions to the scattering of electrons from polyatomic molecules (Gianturco and Stoecklin 1994). Finally, we note that because the study of Malegat *et al* was restricted to eigenphase sums, it did not demonstrate the extent of the duplicitous convergence behaviour which we have found that cross sections can display when calculated from a separable representation (see section 3).

In section 2 we provide details of the method used to solve the electron–molecule scattering equations, focusing on the details of the basis sets used to construct a separable expansion of the exchange kernel. Section 3 contains a presentation and description of selected eigenphase sums and cross sections (partial, total and differential) for the equilibrium geometry (bond length) of H_2. Section 4 focuses on the general lessons learned regarding the selection of exchange basis sets. These conclusions should be extendible to calculations of polyatomic molecules as well as underpinning more complicated formulations of exchange such as the Schwinger separable representation (McCurdy and Rescigno 1992).

2. Method

The goal of the present work is to determine the viability of using a separable representation of the exchange potential in calculations of *ab initio* cross sections for low-energy ($E \leqslant 10$ eV), electronically elastic electron–molecule scattering. The hydrogen molecule provides a convenient example of a closed-shell diatomic molecule on which to develop and test our procedures. In the present paper we shall make the additional approximations of 'freezing' the nuclei at their equilibrium separation ($R = 1.4\ a_0$) and of keeping their orientation fixed. With the z-axis coincident with the internuclear vector, this becomes the well known body-frame fixed-nuclei (BF-FN) approximation (e.g. Morrison and Sun 1995, Morrison 1988 and references therein). The time-independent Schrödinger equation then takes the form

$$\left(T_{\rm e} + V_{\rm sp} + \hat{\mathcal{V}}_{\rm ex} - E\right)\psi_E(\boldsymbol{r}) = 0 \tag{1}$$

where $T_{\rm e}$ and E are, respectively, the kinetic energy operator and total energy of the incoming electron. $V_{\rm sp}$ represents the sum of the local static interaction potential and a correlation (polarization) potential. The latter is also taken to be local; it is obtained using linear variational theory in which the incident electron is treated as a fixed point charge (Gibson and Morrison 1984, Morrison and Trail 1993). Specifically, the polarization potential is obtained from the difference between the expectation values of the adiabatic three-electron Hamiltonian for the undisturbed ground state of hydrogen and for the polarized target wavefunction. A larger basis set of nucleus-centred Gaussian-type orbitals is used in the variational calculation for the polarized target. Additionally, a non-penetrating approximation is used to mimic short-range correlation by switching off the repulsive Coulomb interaction between the scattered electron and any target electron whenever the radial coordinate of the latter is larger (Temkin 1957).

2.1. The exchange kernel

The action of the non-local exchange potential operator on the scattering wavefunction may be written in the form

$$\hat{\mathcal{V}}_{\rm ex}\psi_E(\boldsymbol{r}) = \int K(\boldsymbol{r}, \boldsymbol{r}')\psi_E(\boldsymbol{r}')\,{\rm d}\boldsymbol{r}' \tag{2}$$

where, for a closed-shell molecule with $N_{\rm occ}$ occupied orbitals $\xi_i(\boldsymbol{r})$, the exchange kernel is given by

$$K(\boldsymbol{r}, \boldsymbol{r}') = -\sum_i^{N_{\rm occ}} \xi_i(\boldsymbol{r})\frac{1}{|\boldsymbol{r} - \boldsymbol{r}'|}\xi_i^*(\boldsymbol{r}')\,. \tag{3}$$

In the case of molecular hydrogen, there is only one term in the above summation, corresponding to the single bound molecular orbital $\xi_{1\sigma_{\rm g}}$. This is obtained from an SCF calculation, using the POLYATOM electronic structure codes (Moskowitz and Snyder 1977). A (5s2p/3s2p) basis of contracted Gaussian-type orbitals centred on each nucleus is sufficient to yield an electronic energy within 0.07% of the Hartree–Fock limit (Trail *et al* 1990). Furthermore, the associated quadrupole moment at an internuclear separation $R = 1.4\ a_0$ is $0.451\,74e\ a_0^2$, which compares favourably with the experimentally determined value of $(0.474 \pm 0.034)e\ a_0^2$ (Ramsey 1952, Barnes *et al* 1954, Harrick and Ramsey 1952) and the $R = 1.4\ a_0$ value $Q = 0.4568e\ a_0^2$ obtained from configuration-interaction calculations

by Poll and Wolniewicz (1978). As each p-type Gaussian orbital has three Cartesian components, a total of 18 functions are required as input by the electronic structure codes. In this paper, the resulting basis is accordingly designated f18. By way of comparison, the BTAD polarization potential is calculated using a distinct 26-function (6s3p/4s3p) basis, here designated as b26, to represent the polarized molecule.

The exchange kernel can be cast into the separable form

$$K(\boldsymbol{r},\boldsymbol{r}') = \sum_{\alpha\beta} \chi_\alpha(\boldsymbol{r}) K_{\alpha\beta} \chi^*_\beta(\boldsymbol{r}') \tag{4}$$

where the exchange basis functions χ_α are the bound and virtual molecular orbitals determined from a near-Hartree–Fock structure calculation. The symmetry of the exchange basis, characterized by the parity and the projection of the electronic angular momentum on the z-axis, corresponds to that of the scattering wavefunction ψ_E (Trail 1991). Given the SCF coefficients of $\xi_{1\sigma_g}$ and the χ_α, together with the two-electron integrals involving Gaussians, one can determine the exchange expansion coefficients:

$$K_{\alpha\beta} = -\int \chi^*_\alpha(\boldsymbol{r}) \xi_{1\sigma_g}(\boldsymbol{r}) \frac{1}{|\boldsymbol{r}-\boldsymbol{r}'|} \xi^*_{1\sigma_g}(\boldsymbol{r}') \chi_\beta(\boldsymbol{r}')\, \mathrm{d}\boldsymbol{r}\, \mathrm{d}\boldsymbol{r}' . \tag{5}$$

2.2. The exchange basis

A central problem which must be addressed is how to specify precisely the exchange basis functions, χ_α. Because our basis is even tempered, its coverage of the important region of configuration space, the region of the bound target density, is uniform, although not necessarily uniformly convergent. We must accomplish our task without the benefit of a stationary principle to guide us, while at the same time avoiding taking such a large basis that the calculation becomes unwieldy or begins to suffer from linear dependencies. Some consolation is afforded by the knowledge that the expansion in equation (4) must ultimately converge on account of the compact nature of the exchange potential operator (Newton 1982).

It is convenient to begin with the set of molecular orbitals obtained from the SCF calculation of $\xi_{1\sigma_g}$ (Rescigno and Orel 1981). Improved representations of the exchange kernel may then be obtained by performing further SCF calculations using larger numbers of GTOs. In this way we hope to represent adequately the influence of the exchange operator on the occupied molecular orbitals. Several bases were used to expand the χ_α, all of which were obtained by augmenting an initial nucleus-centred basis with GTOs situated on the molecular centre of mass as befits our intention to apply this strategy to vibrational excitation, which entails varying the internuclear separation. Throughout we use normalized Cartesian GTOs of the form (Moskowitz and Snyder 1977, Taketa *et al* 1966, Clementi *et al* 1990)

$$\eta_k(\boldsymbol{r}) = N_{nlm}(\zeta_k) x^l y^m z^n \, \mathrm{e}^{-\zeta_k r^2} . \tag{6}$$

Only s-type ($l+m+n=0$) and p-type ($l+m+n=1$) functions are used both on the nuclei and molecular centre of mass. In order to minimize the likelihood of linear dependence problems while at the same time adequately spanning the exchange region, we impose the following restriction on the choice of exponents of the centre of mass GTOs:

$$\zeta_k = \alpha\beta^k \qquad k = 1, 2, 3 \ldots . \tag{7}$$

Table 1. Gaussian-type orbitals used to construct the exchange bases. Two different starting sets of GTOs have been used, designated (a) f18 and (b) b26. The first s-type GTO is contracted with the contraction coefficients given in parentheses. Details of the centre-of-mass GTOs which are successively added to these starting points are also given. The number of exchange basis functions of different symmetries which can be constructed is given for each Gaussian set. The number of Π_g exchange basis functions is 2 and 3 throughout parts (a) and (b), respectively. $(-n)$ means $\times 10^{-n}$.

		GTO exponents			Size of exchange basis		
(a)	f18	s	$p_{x,y,z}$	Gram determinant	Σ_g	Σ_u	Π_u
		33.644 4 (0.025 374)	2.228	2.30(−6)	5	5	2
		5.057 96 (0.189 683)	0.518 3				
		1.146 8 (0.852 93)					
		0.321 144					
		0.101 309					
	f22	0.04	0.01	3.13(−7)	6	6	3
	f26	0.02	0.005	3.14(−10)	7	7	4
	f30	0.01	0.002 5	3.55(−14)	8	8	5
	f34	0.005	0.001 25	1.46(−18)	9	9	6
	f37		0.02	6.18(−22)	9	10	7
	f40		0.04	6.49(−26)	9	11	8
	f43		0.08	1.58(−31)	9	12	9
	f46		0.16	2.45(−37)	9	13	10
(b)	b26						
		33.644 4 (0.025 374)	1.114 2	3.10(−15)	7	7	3
		5.057 96 (0.189 683)	0.259 2				
		1.146 8 (0.852 93)	0.06				
		0.321 144					
		0.101 309					
		0.03					
	b42	0.04	0.01	2.19(−32)	11	11	7
		0.02	0.005				
		0.01	0.002 5				
		0.005	0.001 25				
	c42	0.04	0.01	6.55(−25)	11	11	7
		0.013 333 33	0.003 333 33				
		0.004 444 44	0.001 111 11				
		0.001 481 48	0.000 370 37				

Such a geometrical progression of the exponents leads to our basis set being systematically augmented in an 'even-tempered' fashion (Dunning and Hay 1977, Wilson 1983). Details of the GTO bases used in the present paper are given in table 1. Calculations have been performed with both the static potential basis (f18) and the polarization basis (b26) as starting points. In the latter case, the two augmented bases (b42 and c42) were chosen with the intention of investigating the sensitivity of the scattering calculations to the ratio, β, of the geometrical progression (7).

For each GTO basis in table 1 we also quote the value of the Gram determinant for the fixed internuclear distance of 1.4 a_0. Its utility arises from the fact that for a linearly independent basis $\{\eta_k(\boldsymbol{r})\}$, the Gram determinant satisfies the condition (Cushing 1975)

$$\det\{S_{ij}\} \equiv \det\left\{\int \eta_i(\boldsymbol{r})\eta_j(\boldsymbol{r})\,\mathrm{d}\boldsymbol{r}\right\} > 0\,. \tag{8}$$

If, however, the Gram determinant is zero, then the basis from which it was constructed is linearly dependent. Numerically, this theorem translates into a guideline: the smaller

the Gram determinant, the more nearly linearly dependent the basis. For this reason, the Gram determinant is a useful, though numerically imprecise, measure of linear independence (Löwdin 1956).

Although the Gram determinant may depend on the size of the basis, it is especially meaningful in comparing bases of equal dimension. Thus, the Gram determinants for the bases f18–f46 decrease as the basis size increases. But the b42 and c42 basis sets contain the same number of Gaussians, and the Gram determinant of the latter is much larger. This is a consequence of the smaller overlap, S_{ij}, between adjacent centre of mass GTOs. For even-tempered GTOs, the overlap between adjacent functions in the series depends on the function type and the ratio of the geometrical progression, β. As an example, for s-type functions, this overlap is 0.91 and 0.81 in the b42 and c42 cases, respectively.

Any irregularities in the behaviour of the Gram determinant with basis set could be indicative of the onset of approximate linear dependence arising from the finite precision of the computations. If required, more detailed information may be obtained by examining the individual eigenvalues of the overlap matrix, the smallest of which also provides a measure of linear independence (Löwdin 1967, Nordling 1975). Note that the form of the non-local exchange operator (Morrison 1988)

$$\hat{\mathcal{V}}_{\rm ex} = -\sum_{i=1}^{N_{\rm occ}} |\xi_i\rangle \hat{\mathcal{V}}^{\rm ee} \langle \xi_i| \tag{9}$$

where $\hat{\mathcal{V}}^{\rm ee}$ is the two-electron repulsion operator with coordinate space projection

$$\langle \boldsymbol{r}|\hat{\mathcal{V}}^{\rm ee}|\boldsymbol{r}'\rangle = \frac{1}{|\boldsymbol{r}-\boldsymbol{r}'|} \tag{10}$$

ensures that $\hat{\mathcal{V}}_{\rm ex}$ is negative definite (Messiah 1961).

2.3. Eigenvalues of the separable kernel

We effect a further simplification by transforming the exchange basis, χ_α, into one where the kernel is diagonal:

$$K(\boldsymbol{r},\boldsymbol{r}') = \sum_{\gamma}^{N_\gamma} \bar{\chi}_\gamma(\boldsymbol{r})\kappa_\gamma \bar{\chi}^*_\gamma(\boldsymbol{r}')\,. \tag{11}$$

Although this change of representation involves diagonalizing $K_{\alpha\beta}$ in (5), it further simplifies the solution of the Schrödinger equation. Moreover, study of the kernel eigenvalues κ_γ for different basis sets provides useful information on the convergence properties of the expansion (11). The number of terms in the expansion, N_γ, could then be reduced by eliminating kernel eigenvectors $\bar{\chi}_\gamma$ with small eigenvalues (Schneider and Collins 1981b, Malegat *et al* 1987). In the present study all terms are retained.

The kernel eigenvalues for the scattering symmetries $\Sigma_{\rm g}$, $\Sigma_{\rm u}$ and $\Pi_{\rm u}$ are given in tables 2, 3 and 4, respectively. The number of eigenvalues is determined by the number of ways molecular orbitals of the appropriate symmetry can be constructed from the available GTOs. Results are given for all the exchange bases derived from, and labelled by, the GTO

basis sets f18–f46. The f37–f46 bases differ from the f34 by the addition of p-type functions and so contribute only to the Σ_u and Π_u scattering symmetries.

The kernel eigenvalues vary monotonically as more functions are added to the centre of mass, a general behaviour which is independent of whether successive GTOs are more diffuse (f18–f34) or compact (f34–f46). Although the first five eigenvalues of Σ_u symmetry (table 3) appear to have converged for the f34 basis, the addition of successively more compact functions (f37–f46) shows this to be an artefact. *Convergence of the kernel eigenvalues in itself is therefore an insufficient indicator of basis set completeness* (Malegat *et al* 1987). Nonetheless, studying the kernel eigenvalues for different basis sets is a useful precursor to a set of scattering calculations. Since the κ_γ are independent of scattering energy their evaluation is computationally much less onerous than the evaluation of cross sections at several energies. The presence of very small ($<10^{-10}$) positive eigenvalues in tables 3 and 4 indicates the limit of numerical precision being reached. Terms in (11) corresponding to negative eigenvalues of smaller magnitude would also be strong candidates for omission.

The exchange kernel eigenvectors may be written in terms of their spherical projections:

$$\bar{\chi}_\gamma(\boldsymbol{r}) = \frac{1}{r}\sum_l \bar{\chi}_{\gamma l}(r) Y_l^\Lambda(\hat{r})\,. \tag{12}$$

For each electron–molecule symmetry we retain the lowest five partial waves, e.g. $l = 0, 2, 4, 6, 8$ in the Σ_g case and $l = 1, 3, 5, 7, 9$ for Σ_u. The partial-wave projected exchange kernel in the body-frame fixed-nuclei approximation is then

$$K_{ll'}^\Lambda(r, r') = \sum_\gamma^{N_\gamma} \bar{\chi}_{\gamma l}(r)\kappa_\gamma \bar{\chi}^*_{\gamma l'}(r')\,. \tag{13}$$

This appears in the familiar radial form of the Schrödinger equation (1):

$$\left[\frac{\mathrm{d}^2}{\mathrm{d}r^2} - \frac{l(l+1)}{r^2} + k^2\right] u_{ll_0}^\Lambda(r) = 2\sum_{l'} V_{ll'}^\Lambda(r) u_{l'l_0}^\Lambda(r) + 2\int \sum_{l'} K_{ll'}^\Lambda(r, r') u_{l'l_0}^\Lambda(r')\,\mathrm{d}r'\,. \tag{14}$$

In equation (14), $V_{ll'}^\Lambda(r)$ are the matrix elements of the local (static or static-polarization) potential. To facilitate their evaluation, the local potential is expanded in terms of Legendre polynomials (Schmid *et al* 1980). Because of the $D_{\infty h}$ symmetry of the homonuclear target, only even-order Legendre polynomials appear in these expansions. For the static and polarization contributions the number of terms retained are four and two, respectively.

It is clear from (14) that improved efficiency in the treatment of the exchange interaction could significantly decrease the time required to solve these equations. The exchange integrals on the right-hand side must be evaluated over the range of the integrand, 'the exchange region', which is roughly the span of the target probability density. Although small compared to the range of the entire interaction, this region contains disproportionately strong non-spherical potentials. So in, for example, propagative algorithms, one must solve for the wavefunction at a large number of positions in configuration space. Often most of the required computing time is consumed with evaluating these integrals. The benefits of using a separable representation of the exchange kernel become more evident when (14) is cast into integral form, the exchange term involving the evaluation of a double integral (Schneider and Collins 1989a). Replacing this with a product of two single integrals makes

Table 2. Eigenvalues of the exchange kernel for symmetry Σ_g. The results demonstrate the variation in the value and number of eigenvalues which may be constructed from the different GTO bases detailed in table 1. The eigenvalues are ordered from left to right by decreasing magnitude and multiplied by -1. $(-n)$ means $\times 10^{-n}$.

Basis	1	2	3	4	5	6	7	8	9
f18	7.15(−1)	1.13(−1)	7.30(−2)	3.07(−2)	8.17(−3)				
f22	7.15(−1)	1.13(−1)	7.34(−2)	3.07(−2)	9.48(−3)	3.67(−4)			
f26	7.15(−1)	1.13(−1)	7.36(−2)	3.07(−2)	1.01(−2)	5.29(−4)	4.48(−6)		
f30	7.15(−1)	1.13(−1)	7.37(−2)	3.07(−2)	1.04(−2)	6.03(−4)	8.04(−6)	5.64(−8)	
f34	7.15(−1)	1.13(−1)	7.37(−2)	3.07(−2)	1.05(−2)	6.39(−4)	1.02(−5)	1.15(−7)	1.16(−10)

Table 3. As table 2 but for Σ_u scattering symmetry.

Basis	1	2	3	4	5	6	7	8	9	10	11	12	13
f18	1.92(−1)	6.32(−2)	3.28(−2)	1.29(−2)	3.48(−3)								
f22	1.92(−1)	6.32(−2)	3.28(−2)	1.30(−2)	3.55(−3)	9.36(−6)							
f26	1.92(−1)	6.32(−2)	3.28(−2)	1.30(−2)	3.59(−3)	1.49(−5)	3.81(−9)						
f30	1.92(−1)	6.32(−2)	3.28(−2)	1.30(−2)	3.60(−3)	1.77(−5)	6.90(−9)	4.27(−13)					
f34	1.92(−1)	6.32(−2)	3.28(−2)	1.30(−2)	3.61(−3)	1.90(−5)	8.66(−9)	4.53(−13)	−5.48(−12)				
f37	1.92(−1)	6.32(−2)	3.29(−2)	1.33(−2)	3.92(−3)	6.45(−5)	1.49(−7)	6.79(−11)	5.06(−15)	−6.46(−12)			
f40	1.92(−1)	6.33(−2)	3.32(−2)	1.40(−2)	4.63(−3)	1.80(−4)	1.84(−6)	4.51(−9)	4.32(−12)	8.33(−16)	−7.60(−12)		
f43	1.92(−1)	6.36(−2)	3.39(−2)	1.51(−2)	5.88(−3)	4.23(−4)	2.71(−5)	9.18(−7)	3.00(−9)	1.23(−12)	3.48(−17)	−8.11(−12)	
f46	1.92(−1)	6.40(−2)	3.50(−2)	1.70(−2)	7.04(−3)	1.24(−3)	3.13(−4)	2.17(−5)	2.57(−7)	6.39(−10)	2.88(−13)	1.84(−15)	−8.41(−11)

Table 4. As table 2 but for Π_u scattering symmetry.

Basis	1	2	3	4	5	6	7	8	9	10
f18	1.28(−1)	4.05(−2)								
f22	1.28(−1)	4.05(−2)	1.12(−4)							
f26	1.28(−1)	4.05(−2)	1.85(−4)	4.00(−8)						
f30	1.28(−1)	4.05(−2)	2.23(−4)	7.29(−8)	4.02(−12)					
f34	1.28(−1)	4.05(−2)	2.41(−4)	9.18(−8)	6.62(−12)	−1.34(−12)				
f37	1.28(−1)	4.05(−2)	9.46(−4)	1.69(−6)	6.73(−10)	3.37(−14)	−2.38(−12)			
f40	1.28(−1)	4.05(−2)	2.75(−3)	2.24(−5)	4.21(−8)	1.83(−11)	1.01(−15)	−2.58(−12)		
f43	1.28(−1)	4.05(−2)	5.77(−3)	1.87(−4)	1.70(−6)	3.66(−9)	1.65(−12)	1.32(−16)	−2.97(−12)	
f46	1.28(−1)	4.07(−2)	9.25(−3)	9.59(−4)	4.15(−5)	4.59(−7)	1.11(−9)	4.67(−13)	4.03(−17)	−3.16(−12)

the corresponding Gaussian quadratures both simpler to program and quicker to evaluate (Schneider and Collins 1981b). This is an important consideration given that the evaluation of the exchange kernel, in the present work, would otherwise account for at least half of the computer time taken for a scattering calculation at a single energy. Even more CPU time is required for targets with more than one occupied orbital.

All of the calculations reported here obtained $u^{\Lambda}_{ll_0}(r_\beta)$ on a variable 55-point mesh between 0 and 10 Bohr by the solution of a set of linear algebraic equations (Schneider and Collins 1989a, b). Similar implementations of this linear algebraic method were used for both the separable exchange and benchmark exact exchange calculations reported in the present paper. For each of the four electron–molecule symmetries (Σ_g, Σ_u, Π_u and Π_g), we retained the six lowest channels, l. At a radial separation of 10 Bohr, the scattering functions were used to construct a five-channel R-matrix, $\boldsymbol{u}(r)\left\{\frac{\mathrm{d}}{\mathrm{d}r}\boldsymbol{u}(r)\right\}^{-1}$. This was then propagated out to a distance of 170 Bohr where the reactance matrix $K^{\Lambda}_{ll'}$ was finally obtained. This combination of the linear algebraic and R-matrix propagator methods exploits the qualitative difference in the strength of the interaction potential at short and long range.

3. Results

Starting from the reactance (or K-) matrix we have obtained eigenphase sums and then integrated cross sections based on body-frame/fixed-nuclei transition (or T-) matrices. Rotationally-resolved differential cross sections were also obtained at 35 scattering energies ranging from 0.0469 to 10 eV, the former lying just above the threshold (0.0439 eV) for the $j = 0 \rightarrow j' = 2$ rotational excitation. For energies below 2 eV, the first Born approximation is used to scale the K-matrix elements in a way which ensures that the rotationally inelastic cross sections obey the correct threshold law. Further details on this SANR (scaled adiabatic nuclear rotation) method have been given by Feldt and Morrison (1984) and Morrison and Sun (1995).

3.1. Eigenphase sums

Malegat *et al* (1987) showed that the eigenphase sum will, in general, behave in an oscillatory fashion with respect to the number of terms included in the separable expansion of exchange. They observed monotonic behaviour with respect to the addition of eigenvectors, $\bar{\chi}_\gamma$, with successively smaller eigenvalues, κ_γ; but this depends on retaining throughout the same basis of atomic orbitals. This convergence property, derived by Malegat et al at the static-exchange level, would provide a useful way of minimizing the number of terms in the exchange expansion (13) once a sufficiently complete atomic orbital basis has been identified. The latter is the particular focus of the present work.

In tables 5 and 6 we present eigenphase sums for, respectively, the Σ_u and Π_u electron–molecule symmetries. Results are quoted at the static-exchange-polarization (SEP) level for the nine basis sets f18–f46. Exact, i.e. non-separable, exchange results are also given for the two sample scattering energies: 3 and 8 eV (see also Trail and Morrison 1995). Static-exchange (SE) values are given for the f46 basis to illustrate the importance of including polarization and to provide a point of comparison with other work. As expected, the inclusion of the attractive polarization interaction yields arithmetically higher eigenphase sums for all four electron–molecule symmetries and at all 35 energies studied.

A striking feature of table 5 is the insensitivity of the Σ_u eigenphase sum to the number of GTO basis functions. We found this to be the case for all energies studied. Furthermore, all three GTO bases originating in polarization studies (b26, b42, c42) yielded eigenphase sums

Table 5. Σ_u eigenphase sums (SEP).

Basis	$E = 3$ eV	$E = 8$ eV
f18	0.619	1.075
f22	0.619	1.072
f26	0.619	1.071
f30	0.619	1.070
f34	0.619	1.069
f37	0.617	1.060
f40	0.618	1.052
f43	0.620	1.058
f46	0.620	1.061
Exact	0.622	1.057
SE/f46	0.360	0.810

Table 6. As table 5 but for Π_u scattering symmetry.

Basis	$E = 3$ eV	$E = 8$ eV
f18	0.199	0.420
f22	0.201	0.419
f26	0.202	0.419
f30	0.203	0.419
f34	0.203	0.418
f37	0.219	0.419
f40	0.241	0.425
f43	0.234	0.443
f46	0.234	0.440
Exact	0.235	0.441
SE/f46	0.101	0.263

(not shown) which were effectively coincident (to graphical precision) with the results for the f46 basis. Given the dominant role played by the Σ_u symmetry in rotational excitation (e.g. Trail *et al* 1990), this is encouraging. At the same time an exclusive reliance on the eigenphase sum as a measure of convergence can be misleading (Morrison 1979). Partial cross sections appear to be a more sensitive and reliable measure in addition to being closer to the physical observables of interest.

The analogous convergence tests for the Π_u symmetry (table 6) demonstrate a greater sensitivity to the basis used to construct the exchange eigenfunctions. Inspection of the results for the f18–f34 bases might have encouraged the erroneous conclusion that convergence had been achieved. However, enhancement of the f34 basis with more compact GTOs (f37–f46) was necessary to reproduce the benchmark result obtained by treating exchange directly. Without a suitable variational principle as a guide, it is clearly necessary to design a procedure for choosing a basis set which minimizes the risk of falling prey to this 'duplicitous pseudo-convergence'. We further note that the eigenphase sum does not, in general, behave monotonically with respect to increasing the size of the Gaussian basis.

As with the Σ_u eigenphase sums, we found for the Π_u symmetry that basis sets containing additional diffuse nucleus-centred GTOs (b26, b42, c42) yielded similar values (not shown). In this case, however, the difference between these and the f46 (and hence exact) eigenphase sums became noticeable for energies above 6 eV. Evidently the addition of more compact centre-of-mass functions was important in modelling the short-range behaviour of the exchange kernel. Interestingly, this proved not to be the case for the

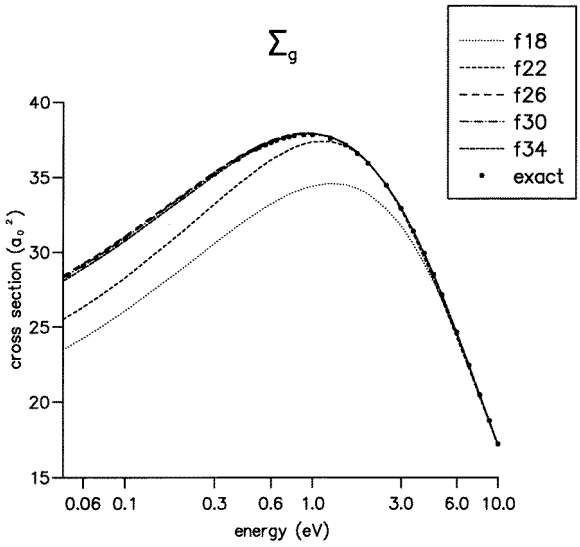

Figure 1. Dependence of the Σ_g partial cross section on the number of Gaussian-type orbitals used to construct the exchange basis. f18 represents the same, nucleus-centred, basis used to evaluate the static potential. For this symmetry, the successive addition of more diffuse s-type GTOs on the centre of mass is responsible for the differences in the cross sections obtained with the larger bases. Benchmark cross sections obtained with an 'exact', i.e. properly non-separable, representation of exchange are shown as full circles.

Σ_g symmetry, where all calculations (f18–f34, b26, b42, c42) agreed satisfactorily with the exact results.

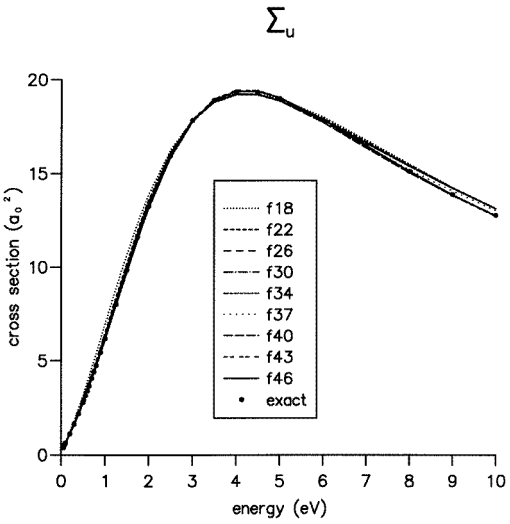

Figure 2. Dependence of the Σ_u partial cross section on the number of GTOs used to construct the exchange basis. The curves for f22–f34 show the effect of adding successively more diffuse p-type GTOs on the centre of mass. The behaviour of the f37–f46 cross sections arises from the addition of more compact GTOs on the centre of mass. Exact results are shown as full circles.

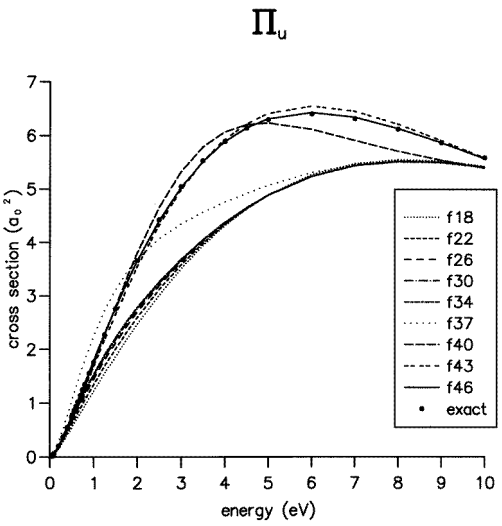

Figure 3. As figure 2, but for the Π_u scattering symmetry. Again, it is p-type centre-of-mass GTOs which are responsible for the observed differences between the separable exchange calculations.

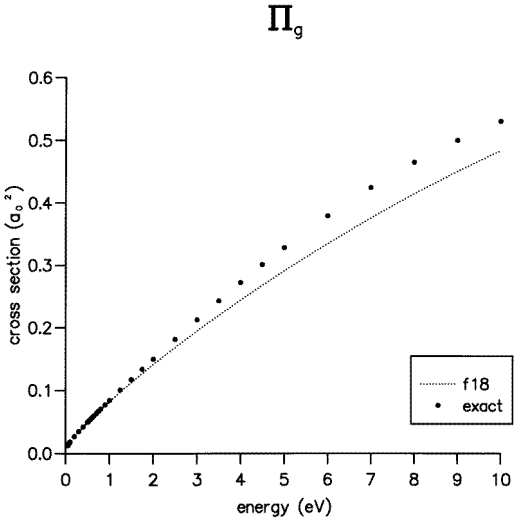

Figure 4. Determination of the Π_g partial cross section using the f18 GTO basis, from which two symmetry-adapted exchange eigenfunctions may be constructed. Non-separable results are shown as full circles.

3.2. Partial cross sections

Figures 1–4 show how the body-frame partial cross sections vary with the GTO basis used to expand the exchange eigenfunctions. The 'exact' cross sections, which are also shown, were obtained by direct evaluation of the exchange kernel without the intermediate step of a separable expansion.

In the case of the Σ_g cross section, the addition of two centre-of-mass GTOs (to give

the f26 basis) is sufficient to achieve good agreement with the exact-exchange results even at the lowest scattering energies. This is particularly significant in the context of the Σ_g symmetry, which has no centrifugal barrier in the lowest partial-wave channel. At higher energies the exchange interaction should become relatively less important as the integrand in (2) includes a more oscillatory function ψ_E. Nonetheless, even at 10 eV the Σ_g cross section at the (f46) static-exchange level (17.11 a_0^2) is much closer to the analogous result for the complete interaction (17.15 a_0^2) than are the cross sections for the static-polarization (15.72 a_0^2) and static (14.58 a_0^2) potentials. Only results for the complete interaction appear in figures 1–4. Similar comparisons attest to the importance of the exchange interaction at all the other (lower) energies studied.

Figure 2 demonstrates that the Σ_u cross section is far less sensitive than the Σ_g cross section, and is fairly well converged for all basis sets, though significant percentage deviations from the exact result will inevitably occur at lower energies where the cross section is small. At higher energies, there are indications that two of the more compact centre-of-mass GTOs are needed, i.e. that f40 is the smallest basis that yields consistently accurate cross sections. For energies up to about 1.5 eV we also found that both the polarization and exchange interactions play an important role in the scattering process for this symmetry. However, the static-polarization (SP) results came closer than the static-exchange (SE) to the cross section for the full interaction (SEP). This is a consequence of the centrifugal barrier inhibiting exposure of the scattering electron to the exchange interaction, in comparison with polarization effects which are of longer range. Above 1.5 eV the SE results are closest to the SEP, but remain significantly lower for all energies studied. At 10 eV, for example, the SE partial cross section is 9.81 a_0^2, compared to 12.74 a_0^2 for the full interaction.

The (smaller) partial cross sections in the Π_u symmetry (figure 3) provide a clear amplification of many of the points which have been raised so far. That these are much more sensitive to the exchange basis than the analogous Σ_u partial cross sections, which admit the same partial-wave orders ($l = 1, 3, 5, 7, 9$), could be attributable to two effects. Firstly, the matrix elements of the interaction potential differ, in this case because of the different values of the projection of l on the internuclear axis. Second, the description of the exchange kernel afforded by a nucleus-centred basis is likely to be less complete in the region of configuration space covered by the centre-of-mass p_x and p_y GTOs which contribute to the Π_u calculations.

For the Π_u symmetry only the f43 and f46 bases, containing the most compact centre-of-mass GTOs, lead to acceptable agreement with the benchmark results. The f18–f34 sequence of basis sets, derived by successively including more diffuse GTOs, provides a misleading appearance of convergence. This pseudo-convergence is slowest at energies below 4 eV where exchange effects near the fringe of the target charge cloud are emphasized. The number of more compact functions provided by the f37 and f40 bases is inadequate to bridge the gap between the f34 and benchmark results, most notably at the higher, more penetrating, energies. A comparison of Π_u partial cross sections obtained using only the static (S) potential, as well as the SE, SP and SEP models, was also performed. As in the Σ_u case, both the SP and SE cross sections were significantly smaller than the full (SEP) results, with the SP being closer for lower energies (below 3.5 eV). For both these symmetries, the purely static potential gives much the smallest cross sections for all energies above the near-threshold region.

For the Π_g symmetry the SP cross sections are closest to the SEP model at all energies studied. This should not be too surprising in view of the relatively large centrifugal barrier effects (the lowest-order partial wave in this symmetry is $l = 2$) and the absence of any

resonance structure. The relative unimportance of exchange for this symmetry can also be seen in figure 4. The f18 calculation, which allows the construction of only two symmetry-adapted exchange eigenfunctions, agrees acceptably well with the exact results. Our decision not to fully converge the small Π_g partial cross sections could compromise the accuracy of some differential cross sections, particularly those for excitation processes. However, it is clearly not a material consideration for the determination of the total integrated cross section considered in the next section.

3.3. Total cross sections

Summing the partial cross sections from the preceding subsection, we obtain total integrated cross sections which, in the body-frame/fixed-nuclei approximation, include the elastic contribution and (adiabatically) all rotational excitations. Table 7 gives the total cross sections for different exchange bases at nine representative scattering energies. Although the Σ_g partial cross section is the largest at all energies studied, the sum is significantly influenced by the Σ_u and Π_u symmetries particularly above about 2 eV.

In general, the f46 cross sections are closest to the exact results in the final column. At energies below 1 eV, the diffuse centre-of-mass functions of the f34 basis provide for an adequate representation of exchange. In fact, the f34 and f46 results agree to four significant figures for energies up to 0.3 eV. This is a consequence of our using the same numerical parameters throughout this study rather than an indicator of the precision of the work, which is about 1% for total cross sections.

At intermediate energies (between about 1 and 5 eV) the b42 and c42 bases perform as well as f46. Their relative failure at higher energies is to be expected as a result of their relatively more diffuse nature. Similar discrepancies exist at the lowest scattering energies where the Σ_g symmetry dominates. Of more interest is the close agreement between the b42 and c42 results which illustrates insensitivity to the choice of the geometric progression ratio (respectively $\frac{1}{2}$ and $\frac{1}{3}$) defining the even-tempered part of the basis. The more compact b42 basis generally gives marginally better agreement with the exact results for energies above about 2 eV.

For energies up to 7 eV the b26 basis, designed to reproduce the polarization potential, outperforms the f18 from which the static potential is derived. That the f18 basis includes p-type GTOs which are more compact may explain its greater success at energies of 8 eV and above. We mention in passing that BF-FN calculations with an SCF target, such as those in table 7, yield total cross sections in reasonable agreement with experiment. This agreement

Table 7. Total cross sections (a_0^2) for fixed nuclear orientation at nine scattering energies (in eV). These results derive directly from the body-frame/fixed-nuclei K-matrix to which no 'SANR' scaling has been applied. Within the adiabatic nuclear rotation approximation, these values equal the sum of the rotationally elastic and all inelastic cross sections.

Energy	f18	f34	f46	b26	b42	c42	Exact
0.05	24.12	28.74	28.74	27.24	27.86	27.88	28.92
0.30	32.73	37.19	37.19	36.32	36.52	36.56	37.26
1.00	42.66	45.73	45.89	46.08	45.68	45.74	45.84
2.00	50.37	52.30	52.95	53.08	52.99	53.01	52.99
3.00	53.33	54.70	56.00	55.61	56.01	56.00	56.04
5.00	50.98	51.20	52.79	52.44	52.76	52.81	52.77
7.00	45.00	44.83	45.59	46.10	46.04	46.12	45.66
8.00	41.89	41.74	42.08	42.89	42.77	42.84	42.19
10.00	36.19	36.16	35.94	36.93	36.90	36.92	36.08

improves significantly when vibrational averaging of the H_2 motion is taken into account (Trail *et al* 1990).

3.4. Rotational excitation

The body-frame/fixed-nuclei (BF-FN) calculations reported in this paper derive from a composite of the fixed-nuclear-orientation (FNO) and rigid-rotor approximations in the body-fixed frame of reference. In order to obtain laboratory-frame cross sections for rotational transitions, one has to perform a rotational frame transformation (Chang and Fano 1972, Morrison 1988) on the BF-FN transition matrix. The latter is related to the K-matrix which may be scaled using the SANR method (Feldt and Morrison 1984) for near-threshold energies, thereby compensating for the main deficiency of this adiabatic approach: violation of threshold laws because of the neglect of the molecular rotation Hamiltonian. It is important to note that the adiabatic nuclear rotation cross sections obtained from the rotational frame transformation do not go to zero at threshold and so a SANR (or some comparable) correction is essential for scattering at very low energies.

In addition to its use in the SANR method to provide necessary scaling of the K-matrices, the Born approximation is also used to obtain K-matrix elements for both higher partial waves and scattering symmetries other than those for which BF-FN close-coupling calculations were performed (Σ_g, Σ_u, Π_u and Π_g). By this judicious combination of close-coupling calculations and the Born approximation we provide, for example, all the BF-FN K-matrices needed for a rotational frame transformation in which H_2 rotor states up to $j = 6$ and total angular momentum $J = 4$ appear. These angular momenta imply a need for eigenvalues of l_z, the projection of l along the internuclear axis, up to 10. Converging the elastic and rotational integrated cross sections to about 1%, however, requires only the Σ and Π symmetries.

Figure 5 shows the integral cross section for purely elastic scattering: $j = 0 \rightarrow j' = 0$. This is qualitatively similar to the Σ_g partial cross section in figure 1, particularly below 1 eV, reflecting the dominance of this symmetry for elastic scattering. As in figure 1, the

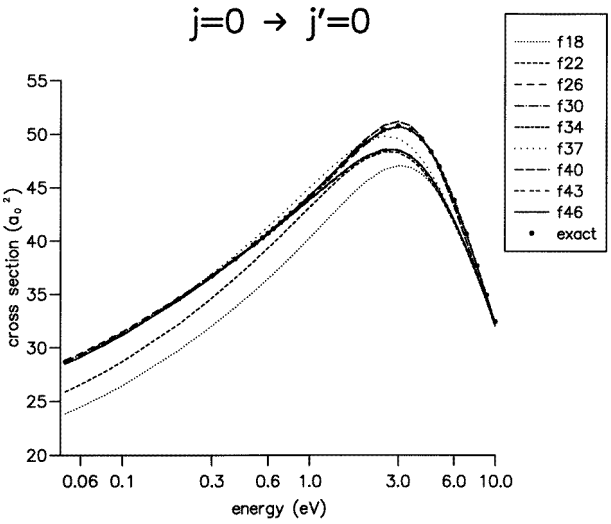

Figure 5. Dependence of the rotationally-elastic integral cross section on the number of GTOs used to construct the exchange basis. Exact, i.e. non-separable exchange, results are shown as full circles.

addition of diffuse centre-of-mass functions converges the separable exchange calculations in the low-energy region. However, the contribution of higher symmetries becomes evident at higher energies through the need to include compact functions in order to bring the separable exchange calculations in line with the exact results.

The importance at all energies of the Σ_u and Π_u symmetries is evident in the convergence properties of the integral cross section for rotational excitation $j = 0 \rightarrow j' = 2$ (figure 6). Here the addition of compact centre-of-mass functions is needed to converge the cross section across the entire energy range of interest. The importance of the exchange interaction in general is highlighted by the observation that our static-exchange calculations yield cross sections which are much closer to the complete interaction calculations of figures 5 and 6 than are the analogous static and static-polarization results. The level of agreement is, however, qualitative at best. It is worth noting that the converged integrated cross section for rotational excitation in figure 6 agrees reasonably well with the low-energy (up to 0.5 eV) values derived from the swarm experiments of Crompton and co-workers (Morrison *et al* 1987). The level of agreement improves substantially when one rigorously includes the influence of molecular vibration (Trail 1991).

3.5. Differential cross sections

The use of the Born approximation to provide transition matrix elements corresponding to higher partial waves is particularly important when calculating differential cross sections (DCS) for rotationally inelastic processes (Morrison *et al* 1984). Both the long-range form of the polarization interaction as well as the contribution from the permanent quadrupole of H_2 are included in our determination of the first Born approximation T-matrix elements. As discussed in section 3.4 above, these supplement those T-matrix elements corresponding to lower partial waves which are obtained via body-frame close-coupling calculations using the full interaction potential (equation (14)).

In figure 7 we show the differential cross section for the elastic scattering process $j = 0 \rightarrow j' = 0$, where the energy of the incident electron is 3 eV. In addition to the

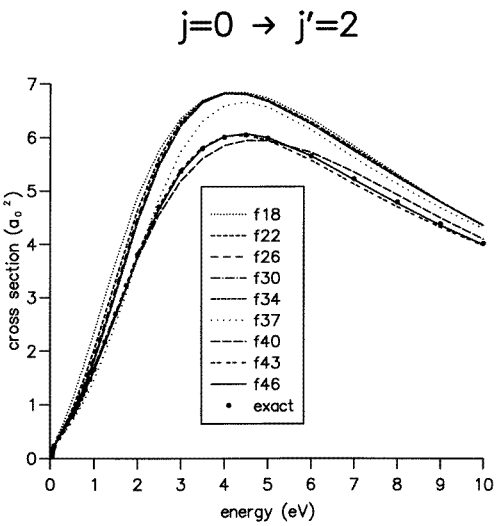

Figure 6. Dependence of the rotationally-inelastic, $j = 0 \rightarrow j' = 2$, integral cross section on the number of GTOs used to construct the exchange basis. Results obtained with a non-separable treatment of exchange are shown as full circles.

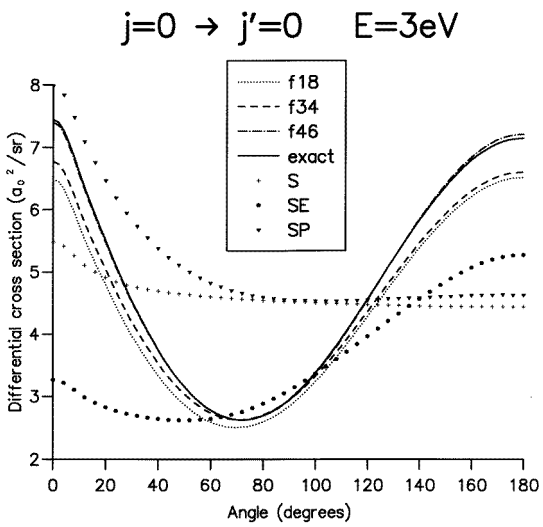

Figure 7. Differential cross section for elastic scattering, $j = 0 \rightarrow j' = 0$, at an incident electron energy of 3 eV. Results are given for three exchange basis sets (f18, f34, f46) and for exact (non-separable) exchange. The importance of different contributions to the interaction potential is illustrated by the displayed results obtained using only the static interaction (S), the static and exchange interactions (SE), and the static and polarization interactions (SP).

'exact' results obtained by a fully non-separable treatment of exchange, we display the outcome of calculations using three of our exchange basis sets: those labelled f18, f34, f46. These show the influence of enhancing an SCF basis (f18) with successively diffuse (f34) and then compact (f46) centre-of-mass functions. The figure also shows the effect of omitting certain contributions to the electron–molecule interaction potential: calculations have been performed using a purely static potential, as well as ones omitting either the exchange or polarization potentials.

Although all three exchange basis sets give the correct general shape for the SEP differential cross section at 3 eV, the inclusion of the more compact functions is necessary to yield quantitative agreement with the exact results over all scattering angles. The addition of diffuse centre-of-mass functions is important in the region of the minimum of the DCS, but much less important at larger scattering angles. Back scattering at this energy is influenced more by the addition of compact functions to represent exchange, an indication of the degree to which the scattered electron penetrates the molecular charge cloud. It is interesting that one can obtain a reasonable result for the forward scattering DCS even when exchange is omitted entirely from the calculation, as seen from the static-polarization results of figure 7. This illustrates the relative importance of the long-range potential in determining low-angle scattering. Though one has to include all contributions to the potential to obtain the back scattering DCS, the static-exchange results are significantly better in magnitude and shape than the static polarization.

For an energy of 10 eV (not shown), the static-exchange elastic DCS was found to be more realistic than the static-polarization (and static) results for all but the lowest ($\lesssim 14^\circ$) scattering angles. Although exchange continues to play an important role at this energy, the DCS is insensitive to the exchange basis. Consistent with the diminishing importance of exchange as energy increases is the predominance of forward scattering at 10 eV.

At a low scattering energy like 1 eV, the elastic DCS is more nearly isotropic and peaks

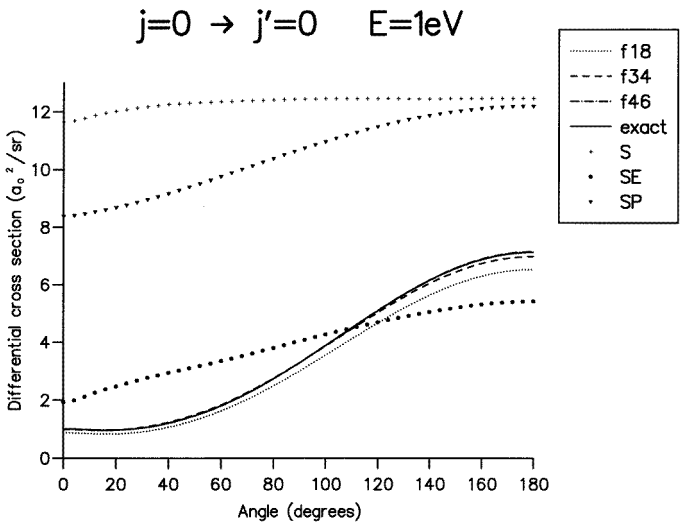

Figure 8. As figure 7, but a scattering energy of 1 eV.

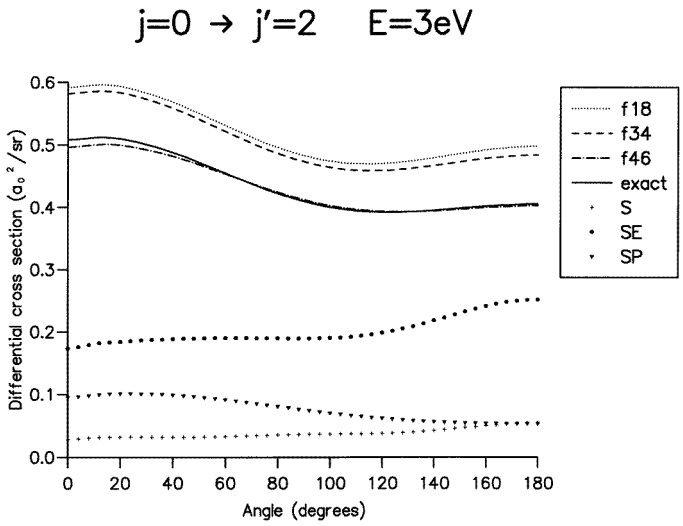

Figure 9. The differential cross section for inelastic scattering, $j = 0 \rightarrow j' = 2$, at an incident electron energy of 3 eV. The calculations illustrated are analogous to those of figure 7.

at 180° and the static-exchange approximation is much better than static polarization at all angles (figure 8). That the f34 exchange basis gives good agreement with the non-separable calculations indicates an increase in the relative influence of the exchange interaction near the fringe of the molecular charge cloud at lower, less penetrating, energies. The situation is similar at very low energies (0.1 eV) except that here the DCS becomes even more isotropic as the collision process begins to resemble atomic S-wave scattering.

Figure 9 shows the differential cross section for rotational excitation, $j = 0 \rightarrow j' = 2$, for an incident scattering energy of 3 eV. At this energy the standard adiabatic nuclear

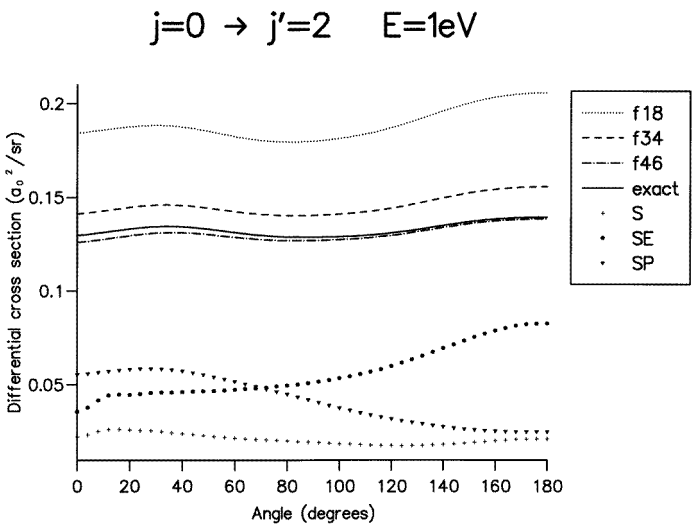

Figure 10. As figure 9, but for an incident electron energy of 1 eV.

rotation method can be used as the important assumption that all rotational states of the molecule are degenerate applies. The DCS is more isotropic than its elastic counterpart (figure 7) and the importance of including more compact functions in the exchange basis is relatively greater. The problem of 'duplicitous pseudoconvergence', illustrated throughout the present paper, was particularly marked for this scattering quantity.

The inelastic DCS for $E = 1.0$ eV (figure 10) shows that diffuse exchange functions are relatively more important at lower energies (cf figure 8 for the analogous elastic DCS). When interpreting rotational excitation DCS for different treatments of the exchange interaction, it may be helpful to bear in mind the competition between short- and long-range effects. The tendency for the torque responsible for rotational excitation to increase with electron–molecule separation will be countered by the weakening of the interaction at longer range (Lane 1980).

We note in passing that for $E < 2$ eV off-diagonal elements of the laboratory-frame reactance matrix $K^J_{jl,j'l'}$, corresponding to $j \neq j'$, have been scaled to correct for deficiencies in the adiabatic nuclear rotation approximation (Feldt and Morrison 1984).

4. Conclusions

The calculations reported in the present paper have been motivated by the widespread use of separable expansions of the exchange interaction in electron–molecule scattering. With increasing attention being paid to the study of polyatomic systems, such expansions seem set to assume still greater relevance (Gianturco *et al* 1995). Using molecular hydrogen as a test case, we have performed several calculations for different exchange basis sets and have compared the results with those obtained using an exact, or non-separable, treatment of exchange. The intention has been to investigate the viability of this representation of the exchange operator and, insofar as possible, to arrive at a prescription for choosing an exchange basis without the benefit of a variational principle as a guide. It is important to appreciate that, however systematic the choice of exchange basis, convergence to the correct

answer cannot be guaranteed. For this reason, benchmark (non-separable) calculations will continue to occupy an important corroborative niche.

Taking the exchange basis as being the bound and virtual molecular orbitals of an SCF calculation, we are left with the choice of a suitable set of atomic orbitals. Mindful of their advantages in polyatomic systems, we take for the latter normalized Cartesian Gaussian-type orbitals. A good starting point is provided by a set of nucleus-centred GTOs designed to recover the near-Hartree–Fock energy of the target molecule, for which an established variational principle exists. This GTO basis can then be supplemented by centre-of-mass functions whose exponents obey a geometrical progression, with a suitable ratio lying between 2 and 3. Using centre-of-mass rather than nucleus-centred functions is advantageous for two reasons. First, this choice minimizes the danger of linear dependence arising from diffuse basis functions. And second, it simplifies calculation of the separable kernel for vibrational excitation calculations, the topic of the forthcoming sequel to this paper. One must also choose a second parameter, α, needed to determine the exponents (see equation (7)). It is worth noting in this context that converged scattering quantities were obtained when the most compact centre-of-mass GTO had an exponent approaching (to within a factor of about 3) that of the most diffuse nucleus-centred function of the same type (s or p).

Because of the empirical nature of this prescription, it is important that one monitors candidate basis sets by evaluating the corresponding eigenvalues of the exchange kernel. The behaviour of the Gram determinant of the GTO set could provide a warning of the onset of linear dependence, though this was not a problem which afflicted any of the present calculations. Though it would in general be clearly impractical to repeat, as here, a series of calculations of scattering quantities for different exchange bases, it may be useful to observe that the differential cross section for rotational excitation seems particularly sensitive.

Even for elastic or rotational excitation cross sections, accurate calculations will require inclusion of molecular vibration. For this reason we have been performing vibrational close-coupling calculations of electron–H_2 scattering using our exchange basis sets. A future paper will examine the extendibility of the separable exchange method, and the utility of our basis sets, for vibrational excitation.

Acknowledgments

We are indebted to Dr L A Collins for stimulating our initial interest in this problem and for performing some early calculations. This work has also benefited from discussions with Dr C W McCurdy. Support for this work came from the US National Science Foundation (NSF grant no PHY-9408977) and many of the calculations were performed on the Cray Y-MP at the National Center for Supercomputing Applications, University of Illinois at Urbana-Champaign.

References

Barnes W R G, Bray P J and Ramsey N F 1954 *Phys. Rev.* **94** 893–902

Buckman S J, Brunger M J, Newman D S, Snitchler G, Alston S, Norcross D W, Morrison M A, Saha B C, Danby G and Trail W K 1990 *Phys. Rev. Lett.* **65** 3253–6

Chang E S and Fano U 1972 *Phys. Rev.* A **6** 173–85

Clementi E, Corongiu G and Chakravorty S 1990 *Modern Techniques in Computational Chemistry: MOTECC-90* ed E Clementi (Leiden: ESCOM) pp 343–434

Collins L A and Morrison M A 1982 *Phys. Rev.* A **25** 1764–7
Collins L A, Robb W D and Morrison M A 1978 *J. Phys. B: At. Mol. Phys.* **11** L777–81
—— 1980 *Phys. Rev.* A **21** 488–95
Collins L A and Schneider B I 1981 *Phys. Rev.* A **24** 2387–401
Crompton R W and Morrison M A 1993 *Aust. J Phys.* **46** 203–29
Dunning T H and Hay P J 1977 *Methods of Electronic Structure Theory* ed H F Schaefer III (New York: Plenum) pp 1–27
Feldt A N and Morrison M A 1984 *Phys. Rev.* A **29** 401–4
Gianturco F A, Rodrigues-Ruiz J A and Sanna N 1995 *J. Phys. B: At. Mol. Opt. Phys.* **28** 1287–300
Gianturco F A and Stoecklin T 1994 *J. Phys. B: At. Mol. Opt. Phys.* **27** 5903–21
Gibson T L and Morrison M A 1984 *Phys. Rev.* A **29** 2497–508
Hara S 1967 *J. Phys. Soc. Japan* **22** 710–8
Harrick N J and Ramsey N F 1952 *Phys. Rev.* **88** 228–32
Jain A, Baluja K L, Di Martino V and Gianturco F A 1991 *Chem. Phys. Lett.* **183** 34–9
Lane N F 1980 *Rev. Mod. Phys.* **52** 29–119
Lovelace C 1964 *Phys. Rev.* B **135** 1225–49
Löwdin P-O 1956 *Advan. Phys.* **5** 1–172
—— 1967 *Int. J. Quant. Chem.* **IS** 811–27
Malegat L and Le Dourneuf M 1988 *J. Phys. B: At. Mol. Phys.* **21** 1237–54
Malegat L, Le Dourneuf M and Vo Ky Lan 1987 *J. Phys. B: At. Mol. Phys.* **20** 4143–62
McCurdy C W and Rescigno T N 1992 *Phys. Rev.* A **46** 255–60
Messiah A 1961 Quantum Mechanics (Amsterdam: North-Holland)
Morrison M A 1979 *Electron–Molecule and Photon–Molecule Collisions* ed T N Rescigno, V McKoy and B I Schneider (New York: Plenum) p 15
—— 1988 *Adv. At. Mol. Phys.* **24** 51–156
Morrison M A and Collins L A 1978 *Phys. Rev.* A **17** 918–38
—— 1981 *Phys. Rev.* A **23** 127–38
Morrison M A, Crompton R W, Saha B C and Petrović Z L 1987 *Aust. J Phys.* **40** 239–81
Morrison M A, Feldt A N and Austin D 1984 *Phys. Rev.* A **29** 2518–40
Morrison M A, Saha B C and Gibson T L 1987 *Phys. Rev.* A **36** 3682–98
Morrison M A and Sun W 1995 *Computational Methods for Electron–Molecule Collisions* eds W M Huo and F A Gianturco (New York: Plenum) pp 131–90
Morrison M A and Trail W K 1993 *Phys. Rev.* A **48** 2874–86
Moskowitz J W and Snyder L C 1977 *Methods of Electronic Structure Theory* ed H F Schaefer III (New York: Plenum) pp 387–411
Newton R G 1982 *Scattering Theory of Waves and Particles (New York: Springer)*
Nordling J O 1975 *Int. J. Quant. Chem.* **IX** 561–81
Poll J D and Wolniewicz L 1978 *J. Chem. Phys.* **68** 3053–8
Ramsey N F 1952 *Phys. Rev.* **87** 1075–9
Rescigno T N, Elza B K and Lengsfield III B H 1993 *J. Phys. B: At. Mol. Opt. Phys.* **26** L567–73
Rescigno T N and Orel A E 1981 *Phys. Rev.* A **24** 1267–71
Schmid G B, Norcross D W and Collins L A 1980 *Comput. Phys. Commun.* **21** 79–90
Schneider B I and Collins L A 1981a *J. Phys. B: At. Mol. Phys.* **14** L101–6
—— 1981b *Phys. Rev.* A **24** 1264–6
—— 1983 *Phys. Rev.* A **27** 2847–57
—— 1989a *Comput. Phys. Rep.* **10** 49–75
—— 1989b *Comput. Phys. Commun.* **53** 381–92
Smith M E, Lucchese R R and McKoy V 1984 *Phys. Rev.* A **29** 1857–64
Taketa H, Huzinaga S and O-ohata K 1966 *J. Phys. Soc. Japan* **21** 2313–24
Temkin A 1957 *Phys. Rev.* **107** 1004–12
Trail W K 1991 *PhD Thesis* University of Oklahoma
Trail W K and Morrison M A 1995 *Phys. Rev.* A submitted
Trail W K, Morrison M A, Isaacs W A and Saha B C 1990 *Phys. Rev.* A **41** 4868–78
Wilson S 1983 *Methods in Computational Molecular Physics* ed G H F Diercksen and S Wilson (Dordrecht: Reidel) pp 71–93
Yamaguchi Y 1954 *Phys. Rev.* **95** 1628–34